BIOCHEMISTRY
including biophysical chemistry & molecular biology

Article

pubs.acs.org/biochemistry

Seeding Specificity and Ultrastructural Characteristics of Infectious Recombinant Prions

Justin R. Piro,[†] Fei Wang,[⊥] Daniel J. Walsh,[†] Judy R. Rees,[‡] Jiyan Ma,[⊥] and Surachai Supattapone*[,†,‡]

[†]Departments of Biochemistry, [‡]Community and Family Medicine, and [§]Medicine, Dartmouth Medical School, Hanover, New Hampshire 03755, United States

[⊥]Department of Molecular and Cellular Biochemistry, Ohio State University School of Medicine, Columbus, Ohio 43210, United States

ABSTRACT: Infectious mouse prions can be produced from a mixture of bacterially expressed recombinant prion protein (recPrP), palmitoyloleoylphosphatidylglycerol (POPG), and RNA [Wang, F.; et al. (2010) *Science 327*, 1132]. In contrast, amyloid fibers produced from pure recPrP without POPG or RNA (recPrP fibers) fail to infect wild type mice [Colby, D. W.; et al. (2010) *PLoS Pathog. 387*, e1000736]. We compared the seeding specificity and ultrastructural features of infectious recombinant prions (recPrP^{Sc}) with those of recPrP fibers. Our results indicate that PrP fibers are not able to induce the formation of PrP^{Sc} molecules from wild type mouse brain homogenate substrate in serial protein misfolding cyclic amplification (sPMCA) reactions. Conversely, recPrP^{Sc} molecules did not accelerate the formation of amyloid *in vitro*, under conditions that produce recPrP fibers spontaneously. Ultrastructurally, recombinant prions appear to be small spherical aggregates rather than elongated fibers, as determined by atomic force and electron microscopy. Taken together, our results show that recPrP^{Sc} molecules and PrP fibers have different ultrastructural features and seeding specificities, suggesting that prion infectivity may be propagated by a specific and unique assembly pathway facilitated by cofactors.

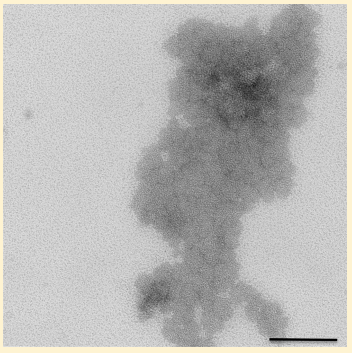

Mammalian prions, the unconventional infectious agents of diseases such as bovine spongiform encephalopathy (BSE), chronic wasting disease (CWD), and scrapie, contain a disease-associated protein termed PrP^{Sc}, which is formed by conformational change from its host-encoded precursor termed PrP^{C}.[3,4] The molecular determinants that are responsible for encoding mammalian prion infectivity are currently unknown, but a series of studies using chemically defined substrates have shown that cofactor molecules are required for infectious prion formation *in vitro*. Synthetic prions displaying levels of specific infectivity (i.e., number of infectious units determined by serial titration bioassay in wild type recipients per molar quantity of protein) similar to those of natural prions can be generated *de novo* using a substrate cocktail containing only native PrP^{C}, copurified endogenous lipids, and a synthetic polyanion.[5] Moreover, prions that infect wild type mice with a rapid incubation period and 100% attack rate can be alternately generated *de novo* using bacterially expressed recombinant PrP (recPrP), synthetic palmitoyloleoylphosphatidylglycerol (POPG), and total liver RNA.[1]

In contrast, various preparations of misfolded recPrP or seeded native PrP^{C} molecules either fail to induce prion disease in wild type hosts[2] or do so with a low level of specific infectivity.[6] Amyloid fibers formed from pure recPrP can induce formation of infectious prions in either a subset of asymptomatic wild type hamsters or symptomatic transgenic mice overexpressing PrP but do not cause prion disease in wild type recipients.[2,7,8] Amyloid is an ordered, cross β-sheet quaternary protein structure that grows by attracting and transforming normal protein conformers through a steric zipper folding mechanism[9,10] and has been implicated in the pathogenesis of diseases involving various tissues throughout the body, such as the heart, brain, and kidney.[11] According to spin-label electron paramagnetic resonance (EPR) studies, the structure of recPrP fibers is predominantly in-register, parallel β-sheet,[12] similar to the structure of yeast prions.[13,14]

In this study, we used several biochemical and ultrastructural assays to compare the seeding specificities and morphological properties of infectious recombinant prions formed by using a mixture of recPrP, POPG, and RNA substrates with those of minimally infectious recPrP fibers formed using recPrP without cofactors. Our results indicate that these preparations differ substantially in both structure and function.

MATERIALS AND METHODS

Reagents. Wild type mice used to make brain homogenate were purchased from Charles River (Wilmington, MA). Monoclonal antibody (mAb) 6D11 was purchased from Covance (Princeton, NJ). Wild type mouse recombinant PrP was expressed in *E. coli* and purified as previously described.[1] Samples of recPrP^{Sc} were produced as previously described.[1] Precleaned Rite-On microslides (3051) were purchased from Gold Seal (Portsmouth, NH). Esco microscope covers 22 × 22, 1.5 thickness were purchased from Erie Scientific (Portsmouth, NH).

Received: May 20, 2011
Revised: July 12, 2011
Published: July 21, 2011

Amyloid Fiber Formation. Amyloid fibers were generated as previously described.[15] Briefly, a 3 mg/mL stock of wild type mouse recombinant PrP was made by adding 6 M GdnHCl to lyophilized protein. A 1.5 mL tube containing a 600 μL reaction volume (2 M GdnHCl, 50 mM MES buffer, pH 6.0, 10 mM thiourea, and 250 μg of recombinant PrP) was incubated at 37 °C with continuous shaking at 1700 rpm for 24 h.

Treatment of Recombinant PrP^{Sc}. Samples of $recPrP^{Sc}$ were treated to remove excess total RNA and digest unconverted recPrP. Tubes containing 1.1 mL of PMCA reactions were thawed, and 15 μL of RNase, DNase Free (Roche, Basel Switzerland) was added. Tubes were incubated at 37 °C while shaking at 350 rpm for 2 h. Material used for the amyloid kinetic seeding assay was treated with 100 μL of a 50% slurry of immobilized TPCK-treated trypsin (catalog # 20230, Thermo Scientific, Rockford, IL). Each tube was incubated overnight with end-over-end rotation in a 37 °C incubator. Samples used for AFM were treated with 5 μg/mL soluble trypsin and incubated overnight with end-over-end rotation in a 37 °C incubator. After incubation tubes containing soluble trypsin received 2 mM PMSF (phenylmethylsulfonyl fluoride) (Roche, Basal Switzerland) while tubes containing immobilized trypsin were spun briefly to pellet the beads. Supernatants were then spun at 100000*g* for 1 h. A 300 μL pellet was left in each tube. To resuspend the pellet, each tube was vortexed for 20 s followed by 2 × 15 s pulses in a Misonix s3000 programmable sonicator equipped with a microplate horn (Misonix, Farmingdale, NY) containing 350 mL of water set at output 85. The concentration of $recPrP^{Sc}$ was determined by comparing Western blot signals to a standard curve made from recombinant amyloid fibers.

Serial Protein Misfolding Cyclic Amplification. Reactions contained 50 μL of 10% perfused brain homogenate made in PBS and 40 μL of conversion buffer (20 mM MOPS pH 7.5, 1% Triton X-100, 500 mM imidazole, 50 mM EDTA and 150 mM NaCl). To initiate the reaction, 10 μL of appropriate normalized seed was added to the first tube of each line. Reaction tubes were subjected to PMCA for 24 h using a Misonix s3000 programmable sonicator equipped with a microplate horn (Misonix, Farmingdale, NY) containing 350 mL of water. Samples were subjected to sonication for 30 s every 30 min at power 75. The temperature was maintained inside the horn by a circulating water bath, pumping warmed water through aluminum coils surrounding the horn. Sample tubes were held in a plastic rack which prevents lid opening and hold tubes ∼3 mm from the surface of the horn. After 24 h, the tubes were removed from the sonicator, and 10 μL of the reaction mixture was added to a new tube containing fresh substrate. SDS-PAGE and Western blotting with anti-PrP antibody 6D11 were performed as previously described.[16]

Atomic Force Microscopy. The samples were imaged with a Veeco Dimension 3100 scanning probe microscope (Veeco, Plainview, NY). All images were captured in tapping mode using a TAP300AL cantilever with a tip radius of <10 nm and a force constant of 40 N/m (Budget Sensors, Sophia, Bulgaria) or with a SSS-NCHR cantilever with a tip radius of <2 nm and a force constant of 42 N/m (Nanosensors, Neuchatal, Switzerland). Each sample (15 μL) was deposited onto a freshly cleaved piece of mica and allowed to dry under a stream of nitrogen for 5 min. Samples were then rinsed with 3 × 150 μL of Millipore water and again allowed to dry under nitrogen for 15 min. Data were collected as 512 × 512 pixel images. Images were subjected to a first-order initial flattening algorithm followed by a first-order plane fit and then a third-order plane fit using the NanoScope 6.12r1 software (Digital Instruments/Veeco, Plainview, NY). These transformations correct for outside noise, noise related to the mica surface, and tilting of the sample stage. The heights of individual aggregates or fibers were measured using the Particle and Pore Analysis Module in the SPIP v5.1.5 software (Image Metrology A/S, Horsholm, Denmark) and using scan sizes <5.0 μm^2. Data were collected using multiple samples, two different tips, and several scanning sessions; >1000 particles or fibers were measured. Data were analyzed using Prism 5.0a (GraphPad Software, La Jolla, CA). AFM images were exported using Gwyddion 2.19 software.

Amyloid Fiber Kinetics. Reactions were made as described above with a few modifications. Each group was performed in triplicate using 460 μL reactions in 500 μL PCR tubes (Axygen, Union City, CA). Prior to incubation, reactions were seeded with 1 μg of preformed recPrP fibers, 1 μg of $recPrP^{Sc}$, or mock seeded with 10 μL of treated cocktail. Samples were incubated for 48 h at 37 °C while continuously shaking at 1700 rpm. At each time point the tubes were briefly vortexed, and a 35 μL sample was removed. Each sample was then diluted with 75 μL of 10 mM sodium acetate buffer pH 5.0 and frozen at −70 °C. After the incubation was finished, the tubes were thawed and 10 μL of thioflavin T (1 mg/mL in 10 mM sodium acetate buffer pH 5.0) was added and vortexed. Samples were scanned as described above with an excitation wavelength of 445 nm and a single emission wavelength of 484 nm. Each sample was replicated three times, scanned ten times, and then averaged. Data were fit to a third-order polynomial function using Prism 5.0a (GraphPad Software, La Jolla, CA).

Transmission Electron Microscopy. Transmission electron microscopy was performed using a JEM-1010 TEM (JEOL Ltd., Tokyo, Japan) operating at 100 kV. Samples were prepared by adsorption of protein to Formvar-coated 300-mesh copper grids for 60 s. Grids were then negatively stained with 2% uranyl acetate for 30 s and allowed to dry overnight before viewing. Images were captured using an integrated AMT digital camera (Advanced Microscopy Techniques, Wobum, MA).

Statistical Analysis. The mean heights and widths of fibers were compared between the two groups by means of two-tailed *t* tests. Descriptive statistics and *t* tests were performed using Stata 10.1 (Stata 10.1. Statacorp, 4905 Lakeway Drive, College Station, TX 77845).

RESULTS

The ability of a protein to template and propagate its misfolded conformation onto natively folded substrate is a unique and fundamental property of infectious prions. We measured this ability using two techniques that autocatalytically propagate differentially folded recombinant PrP structures. Using the serial protein misfolding cyclic amplification (sPMCA) technique, we measured the ability of various preparations to seed PrP^{Sc} formation in native brain homogenates. As expected, sPMCA reactions seeded with brain-derived RML prions propagate protease-resistant, autocatalytic PrP^{Sc} molecules (Figure 1, top blot). Similarly, when sPMCA reactions are seeded with $recPrP^{Sc}$ molecules, we detect conversion of brain homogenate substrate PrP^{C} to PrP^{Sc}, showing that $recPrP^{Sc}$ contains seeding activity in sPMCA reactions (Figure 1, second blot). In contrast, sPMCA reactions seeded with equal amounts of recPrP fibers

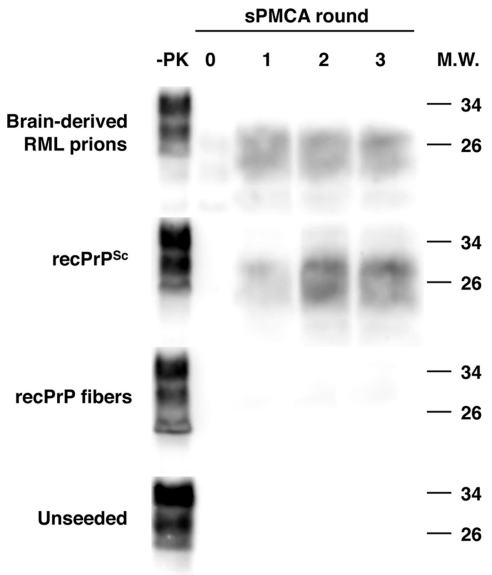

Figure 1. Western blots of sPMCA reactions using normal brain homogenate substrate, seeded with various samples, as indicated. In each blot, the first lane shows the initial round mixture sample not subjected to protease digestion (−PK). The remaining samples were subjected to limited proteolysis with proteinase K.

show no detectable conversion to PrP^{Sc}, similar to unseeded control reactions (Figure 1, third and bottom blots).

We also measured the ability of these various preparations to increase the rate of PrP amyloid formation. We used the dye thioflavin T, which binds to amyloid, to monitor the formation of recombinant fibers. During the course of an unseeded 24 h reaction, we see a characteristic and reproducible increase in thioflavin T fluorescence as fibers are being formed, as previously described[15]

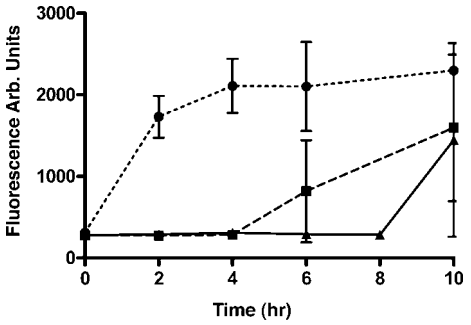

Figure 2. Graph showing the results of the amyloid seeding assay. Samples: (■) mock-seeded; (●) seeded with preformed recPrP fibers; (▲) seeded with $recPrP^{Sc}$. Error bars represent SD.

(Figure 2, squares). When reactions were seeded with a small amount of preformed recPrP fibers, the lag phase is eliminated, demonstrating that recPrP fibers are competent seeds (Figure 2, circles). In contrast, when reactions were seeded with equivalent amounts of $recPrP^{Sc}$, the rate of amyloid formation is delayed when compared to the mock-seeded reaction (Figure 2, triangles versus squares). This result indicates that $recPrP^{Sc}$ does not contain seeding activity in the amyloid fiber assay and delays the rate of PrP fiber formation. The delay caused by $recPrP^{Sc}$ molecules suggests either that they bind to recPrP fibers and prevent their extension (dominant-negative inhibition) or that they affect thioflavin T fluorescence. Taken together, the results of the two complementary assays demonstrate a dichotomy in the seeding capabilities of these two recPrP isoforms: recPrP fibers cannot seed brain homogenate sPMCA reactions while $recPrP^{Sc}$ is unable to seed the formation of PrP amyloid.

We wondered whether structural differences might account for the differences in the templating and propagation activities of $recPrP^{Sc}$ and recPrP amyloid. To study the ultrastructural arrangements and overall morphology of these two PrP isoforms, we utilized tapping mode atomic force microscopy (AFM) and transmission electron microscopy (EM). In AFM imaging, the widths of particles are broadened due to a convolution effect of the AFM probe, but particle heights are accurately measured. Infectious $recPrP^{Sc}$ was found to be comprised of two groups: (a) small puncta and aggregated spherical particles and (b) extended networks of aggregated protein (Figure 3A, right side) with no underlying characteristic

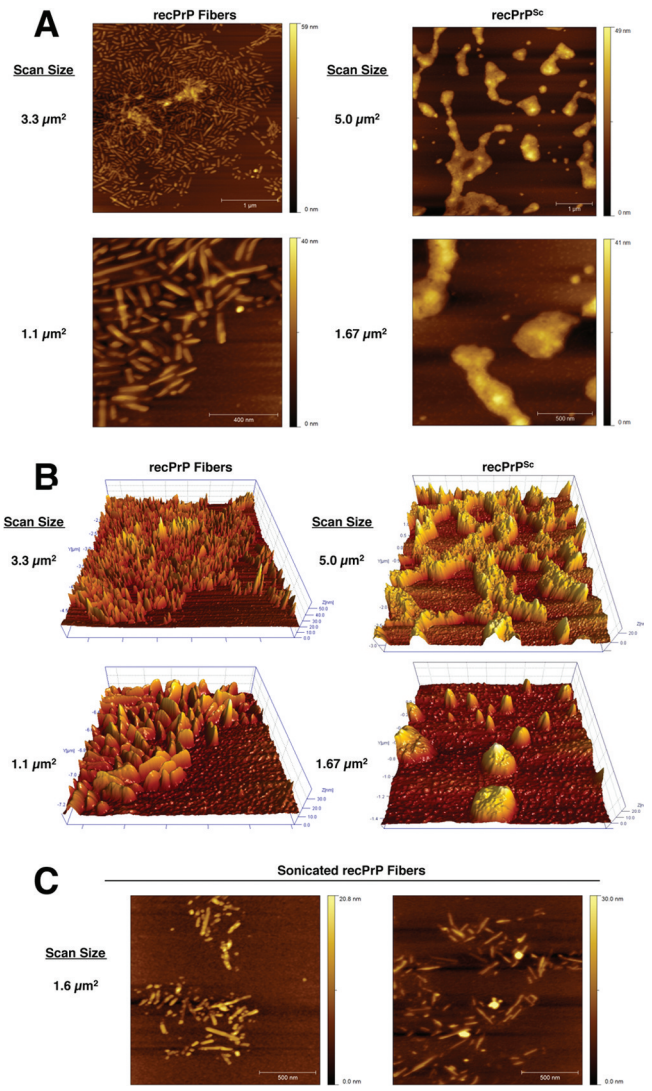

Figure 3. Representative AFM amplitude images. (A) Two-dimensional images of and recPrP fibers (left) and $recPrP^{Sc}$ (right). Images at the bottom are smaller scan sizes captured by using a sharper AFM tip. (B) Three-dimensional images of recPrP fibers (left) and $recPrP^{Sc}$ (right). Images at the bottom are smaller scan sizes captured by using a sharper AFM tip. (C) AFM amplitude images of recPrP fibers treated with a 30 s pulse of sonication before imaging taken from different regions.

dx.doi.org/10.1021/bi200786p | *Biochemistry* 2011, 50, 7111–7116

surface features (Figure 3B, right side). In contrast, recPrP fibers were comprised of elongated structures (Figure 3A, left side) with fiber lengths from 200 to 400 nm, as previously described by Anderson et al.[17] The height of recPrP fibers had a mean of 10.6 nm (N 2397; standard deviation [SD] 5.2; interquartile range [IQR] 6.8−13.6). The height of recPrP^{Sc} aggregates had a mean of 17.4 nm (N 671; SD 9.3; IQR 8.9−23.9). The mean heights in the two groups were significantly different (2-tailed t test, $p < 0.0001$) (Figure 4). As previously

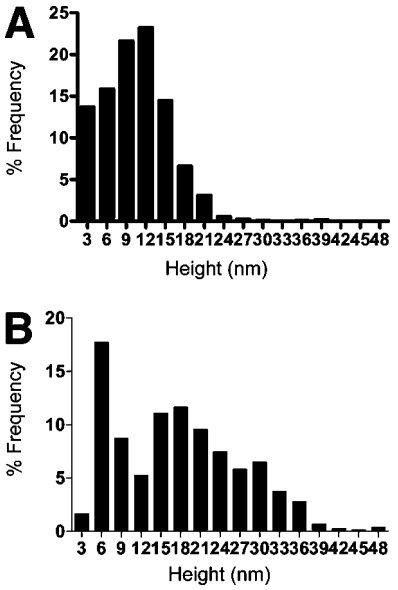

Figure 4. Graphs showing the frequency distribution of heights from either (A) recPrP fibers or (B) recPrP^{Sc}. The data were collected by analyzing AFM images collected in tapping mode. More than 1000 individuals particles were analyzed from each group.

described, some fibers that show a stepwise increase in height (Figure 3B, left side).[17]

During PMCA, samples are subjected to pulses of indirect sonication, and it is possible that sonication-induced physical disruption is responsible for the ultrastructural differences observed between recPrP^{Sc} and recPrP fibers. To investigate this possibility, we subjected recPrP fibers to sonication before imaging in the AFM. The sonicated sample did display some fragmentation, which caused the formation of a few tall aggregates. Nonetheless, the general fiber morphology was retained in sonicated samples, which could be distinguished easily from recPrP^{Sc} samples (Figure 3C). Therefore, the presence of small spherical aggregates and large extended networks combined with the absence of fibers in preparations containing recPrP^{Sc} does not appear to be generated by the sonication step of PMCA alone.

In order to detect any underlying features, we performed negative stain transmission electron microscopy (TEM). When visualized by TEM, recPrP fibers showed characteristic fiber morphology with fiber lengths in good agreement with measurements made by AFM. Some of the imaged recPrP fibers show lateral assembly while at higher magnification a ridge down the long axis of the fibrils can be detected (Figure 5, left side). These surface features are in good agreement with previously published data describing recPrP fibers.[17] TEM images of recPrP^{Sc} molecules show extended networks of aggregates

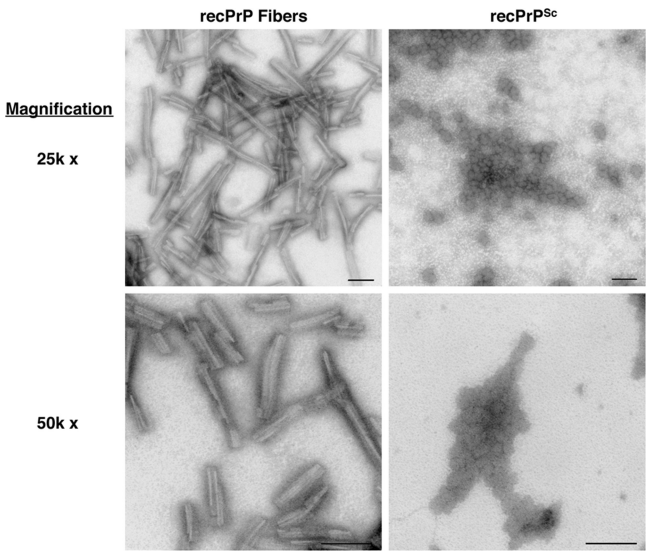

Figure 5. Representative transmission electron microscopic images of recPrP fibers (left) and recPrP^{Sc} (right). Scale bars equal 100 nm.

similar to those detected using AFM. Interestingly, the recPrP^{Sc} aggregates appear to be composed of multiple small spherical oligomers (Figure 5, right side). These oligomers appear to be stuck together in a seemingly random arrangement. Similar to AFM images, individual oligomers can also be found. The width of fibers recPrP fibers had a mean of 16.2 nm (N 204; SD 5.2; IQR 12.0−19.7). The width of recPrP^{Sc} oligomers had a mean of 26.3 nm (N 228; SD 6.3; IQR 21.7−30.4). The mean widths in the two groups were significantly different (2-tailed t test, $p < 0.0001$).

DISCUSSION

The major findings of this report are that infectious recombinant prions differ substantially from noninfectious recPrP amyloid fibers in terms of ultrastructure and seeding specificity. One mechanistic implication of these results is that the relationship between prion infectivity and amyloid formation may not be straightforward, in contrast to other self-propagating proteins such as yeast prions, β-amyloid, and transthyretin.[18] This interpretation is consistent with the variable presence of amyloid plaques in different types of prion disease as well as previous studies in which prion infectivity was retained in preparations of purified brain-derived prions treated with organic solvents that disrupt amyloid structure.[19,20] It is possible that some prion strains are amyloidogenic, but amyloid formation is not fundamentally necessary for prion replication. Alternatively, it is also possible that all prion strains replicate by amyloid formation, but each may have different requirements for this process. Indeed, our experiments do not attempt to exclude the possibility that infectious recombinant prions might be able seed amyloid formation under a different set of experimental conditions. In either case, our results indicate that robust PrP amyloidogenicity and fiber structure are inversely correlated with sPMCA seeding activity or biological infectivity for recombinant prions.[1]

Previously, recPrP fibers have been reported to induce prion disease in transgenic mice overexpressing truncated PrP, but not in wild type mice.[2,7] Since the overexpressors and wild type mice used in these studies share the same genetic background

(FVB) and have similar levels of susceptibility to limiting amounts of infectious prions, it seems unlikely that the discrepancy between the two recipient models in susceptibility to recombinant fibers could be attributed either to the formation of a novel prion strain in overexpressors or inefficient prion propagation in wild type animals. We speculate that recPrP fibers can trigger the formation of nascent, noninfectious PrP amyloid and that this process is facilitated by PrP overexpression. Over the course of the reported two-year incubation period, a subset of nascent PrP amyloid molecules could conceivably interact with endogenous cofactors within the brain to mature into infectious prions that can then be serially transmitted either to overexpressors or wild type recipients. Our finding that recPrP fibers are not able to seed sPMCA reactions using normal mouse brain homogenate substrate is consistent with the conclusion that such fibers are inherently noninfectious, since this assay is several orders of magnitude more sensitive than bioassay,[21] and avoids potential confounders of bioassay such as differential clearance from the brain (recPrP fibers are not degraded after 24 h. PMCA, as determined by Western blot, unpublished observations).[22] However, it is important to note that sPMCA rounds are not sufficient for detecting very small amounts of infectious particles if such were present in the preparations of recPrP fibers.

Our results also suggest that cofactors may play a role in determining the folding pathway of PrP,[23] in this case away from amyloid formation and toward an alternative, infectious structure. If cofactors such as lipids and nucleic acids are able to alter PrP structure, it is possible that they might also influence prion strain properties, which in some cases can be associated with distinct PrP^{Sc} conformations.[24−26] Indeed, reconstitution studies indicate that prions derived from different sources may utilize different classes of endogenous cofactors.[27] More work is required to determine the role played by cofactors in determining the structure and infectious properties of mammalian prions.

The discrepancy in biochemical and ultrastructural properties between recPrP fibers[28] and infectious recombinant prions suggests that the secondary structural arrangements of these two entities may also differ. Spin-label EPR studies revealed that recombinant fibers are primarily composed of parallel, in-register β-sheet structure,[12] similar to the structural arrangement of some yeast prions.[13,14,29] Determining precisely how the structural arrangement of infectious recombinant prions differs from these fibrillar structures may provide valuable information about the molecular basis of prion infectivity.

AUTHOR INFORMATION

Corresponding Author

*Phone: (603) 650-1192. Fax: (603) 650-1193. E-mail: supattapone@dartmouth.edu.

Funding

The National Institutes of Health provided financial support for this study (2R01 NS046478, R01 NS055875, R01 NS060727, and T32 AI007519).

ACKNOWLEDGMENTS

We thank Drs. Ilia Baskakov, Chuck Daghlian, and Harry Higgs for their advice and help with the thioflavin T assay, atomic force microscopy, and fluorescence measurements, respectively.

ABBREVIATIONS

POPG, palmitoyleleoylphosphatidylglycerol; RNA, ribonucleic acid; sPMCA, serial protein misfolding cyclic amplification; BSE, bovine spongiform encephalopathy; CWD, chronic wasting disease; EPR, electron paramagnetic resonance; GdnHCL, guanidine hydrochloride; TPCK, L-1-tosylamido-2-phenylethyl chloromethyl ketone; AFM, atomic force microscopy; PMSF, phenylmethylsulfonyl fluoride; PBS, phosphate buffered saline; MOPS, 3-(*N*-morpholino)-propanesulfonic acid; EDTA, ethylenediaminetetraacetic acid; NaCl, sodium chloride; SDS-PAGE, sodium dodecyl sulfate polyacrylamide gel electrophoresis; PCR, polymerase chain reaction; TEM, transmission electron microscopy; FVB, Friend leukemia virus B.

REFERENCES

(1) Wang, F., Wang, X., Yuan, C. G., and Ma, J. (2010) Generating a Prion with Bacterially Expressed Recombinant Prion Protein. *Science 327*, 1132−1135.

(2) Colby, D. W., Wain, R., Baskakov, I. V., Legname, G., Palmer, C. G., Nguyen, H. O., Lemus, A., Cohen, F. E., DeArmond, S. J., and Prusiner, S. B. (2010) Protease-sensitive synthetic prions. *PLoS Pathog. 6*, e1000736.

(3) Prusiner, S. B. (1982) Novel proteinaceous infectious particles cause scrapie. *Science 216*, 136−144.

(4) Caughey, B., and Raymond, G. J. (1991) The scrapie-associated form of PrP is made from a cell surface precursor that is both protease- and phospholipase-sensitive. *J. Biol. Chem. 266*, 18217−18223.

(5) Deleault, N. R., Harris, B. T., Rees, J. R., and Supattapone, S. (2007) Formation of native prions from minimal componenets in vitro. *Proc. Natl. Acad. Sci. U. S. A. 104*, 9741−9746.

(6) Kim, J. I., Cali, I., Surewicz, K., Kong, Q., Raymond, G. J., Atarashi, R., Race, B., Qing, L., Gambetti, P., Caughey, B., and Surewicz, W. K. (2010) Mammalian prions generated from bacterially expressed prion protein in the absence of any mammalian cofactors. *J. Biol. Chem. 285*, 14083−14087.

(7) Legname, G., Baskakov, I. V., Nguyen, H. O., Riesner, D., Cohen, F. E., DeArmond, S. J., and Prusiner, S. B. (2004) Synthetic mammalian prions. *Science 305*, 673−676.

(8) Makarava, N., Kovacs, G. G., Bocharova, O., Savtchenko, R., Alexeeva, I., Budka, H., Rohwer, R. G., and Baskakov, I. V. (2010) Recombinant prion protein induces a new transmissible prion disease in wild-type animals. *Acta Neuropathol. 119*, 177−187.

(9) Nelson, R., Sawaya, M. R., Balbirnie, M., Madsen, A. O., Riekel, C., Grothe, R., and Eisenberg, D. (2005) Structure of the cross-beta spine of amyloid-like fibrils. *Nature 435*, 773−778.

(10) Kelly, J. W. (2000) Mechanisms of amyloidogenesis. *Nat. Struct. Biol. 7*, 824−826.

(11) Pepys, M. B. (2006) Amyloidosis. *Annu. Rev. Med. 57*, 223−241.

(12) Cobb, N. J., Sonnichsen, F. D., McHaourab, H., and Surewicz, W. K. (2007) Molecular architecture of human prion protein amyloid: a parallel, in-register beta-structure. *Proc. Natl. Acad. Sci. U. S. A. 104*, 18946−18951.

(13) Shewmaker, F., Kryndushkin, D., Chen, B., Tycko, R., and Wickner, R. B. (2009) Two prion variants of Sup35p have in-register parallel beta-sheet structures, independent of hydration. *Biochemistry 48*, 5074−5082.

(14) Wickner, R. B., Dyda, F., and Tycko, R. (2008) Amyloid of Rnq1p, the basis of the [PIN+] prion, has a parallel in-register beta-sheet structure. *Proc. Natl. Acad. Sci. U. S. A. 105*, 2403−2408.

(15) Breydo, L., Makarava, N., and Baskakov, I. V. (2008) Methods for conversion of prion protein into amyloid fibrils. *Methods Mol. Biol. 459*, 105−115.

(16) Piro, J. R., Harris, B. T., Nishina, K., Soto, C., Morales, R., Rees, J. R., and Supattapone, S. (2009) Prion protein glycosylation is not required for strain-specific neurotropism. *J. Virol. 83*, 5321−5328.

(17) Anderson, M., Bocharova, O. V., Makarava, N., Breydo, L., Salnikov, V. V., and Baskakov, I. V. (2006) Polymorphism and ultrastructural organization of prion protein amyloid fibrils: an insight from high resolution atomic force microscopy. *J. Mol. Biol. 358*, 580−596.

(18) Caughey, B. (2000) Transmissible spongiform encephalopathies, amyloidoses and yeast prions: common threads? *Nature Med. 6*, 751−754.

(19) Wille, H., Prusiner, S. B., and Cohen, F. E. (2000) Scrapie infectivity is independent of amyloid staining properties of the N-terminally truncated prion protein. *J. Struct. Biol. 130*, 323−338.

(20) Wille, H., Zhang, G. F., Baldwin, M. A., Cohen, F. E., and Prusiner, S. B. (1996) Separation of scrapie prion infectivity from PrP amyloid polymers. *J. Mol. Biol. 259*, 608−621.

(21) Saa, P., Castilla, J., and Soto, C. (2006) Ultra-efficient replication of infectious prions by automated protein misfolding cyclic amplification. *J. Biol. Chem. 281*, 35245−35252.

(22) Weber, P., Giese, A., Piening, N., Mitteregger, G., Thomzig, A., Beekes, M., and Kretzschmar, H. A. (2007) Generation of genuine prion infectivity by serial PMCA. *Vet. Microbiol. 123*, 346−357.

(23) Supattapone, S. (2010) Biochemistry. What makes a prion infectious? *Science 327*, 1091−1092.

(24) Bessen, R. A., and Marsh, R. F. (1992) Biochemical and physical properties of the prion protein from two strains of the transmissible mink encephalopathy agent. *J. Virol. 66*, 2096−2101.

(25) Telling, G. C., Parchi, P., DeArmond, S. J., Cortelli, P., Montagna, P., Gabizon, R., Mastrianni, J., Lugaresi, E., Gambetti, P., and Prusiner, S. B. (1996) Evidence for the conformation of the pathologic isoform of the prion protein enciphering and propagating prion diversity. *Science 274*, 2079−2082.

(26) Peretz, D., Scott, M. R., Groth, D., Williamson, R. A., Burton, D. R., Cohen, F. E., and Prusiner, S. B. (2001) Strain-specified relative conformational stability of the scrapie prion protein. *Protein Sci. 10*, 854−863.

(27) Deleault, N. R., Kascsak, R., Geoghegan, J. C., and Supattapone, S. (2010) Species-dependent differences in cofactor utilization for formation of the protease-resistant prion protein in vitro. *Biochemistry 49*, 3928−3934.

(28) Bocharova, O. V., Breydo, L., Parfenov, A. S., Salnikov, V. V., and Baskakov, I. V. (2005) In vitro conversion of full-length mammalian prion protein produces amyloid form with physical properties of PrP(Sc). *J. Mol. Biol. 346*, 645−659.

(29) Shewmaker, F., Wickner, R. B., and Tycko, R. (2006) Amyloid of the prion domain of Sup35p has an in-register parallel beta-sheet structure. *Proc. Natl. Acad. Sci. U. S. A. 103*, 19754−19759.